Energy Conversion in Effervescent Atomization

J. Jedelsky*, M. Jicha
Faculty of Mechanical Engineering, Brno University of Technology, Czech Republic
jedelsky@fme.vutbr.cz and jicha@fme.vutbr.cz

Abstract

Atomization of liquids is, from energy point of view, a process of transformation of an input fluid energy into surface energy of produced droplets. We qualitatively describe processes during internal flow, discharge of two-phase mixture as well as spray formation with particular focus to the energy transfer in effervescent atomization. Near nozzle spray visualization elucidates the liquid breakup at different operation modes. General energy equation for steady homogeneous flow is used to explain the energy forms involved in the atomization process. Numerical results illustrate their values and an influence of operational conditions on relations between different energy forms. Main part of the paper is focused on the atomization efficiency. Simple method for estimation of the atomization efficiency of pneumatic atomizers is proposed; surface energy of created droplets, estimated using PDA data, is compared with energy required for the atomization. Atomization efficiency of effervescent atomizers is found to be in fragments of per cents for common operation pressures and gas-to-liquid-ratios (GLRs) and it is inferior by about one order to the efficiency of simple pressure and pressure-swirl atomizers for comparable droplet size. The efficiency declines with both the pressure and GLR with approximately logarithmic tendency.

Introduction

Effervescent atomizers, though relatively new spraying devices, have been already used in a number of practical applications, such as combustion of heavy and waste liquids [1-4], coal-water slurries [5], in gas turbine engines [6], internal combustion engines [7], for spray drying [8], spray coating [9], in process industries [10] and others. Main purpose of atomizers in all these applications is to transform the bulk liquid into fragments or small droplets. This process consumes energy and also other important energy related effects are to be considered when designing or choosing atomizer; e. g. transport of the liquid to target position with some required velocity of droplets, impact and air entrainment. Other requirements, that do not desire energy directly (size distribution/uniformity of droplets, spray steadiness, dispersion of liquid to certain required area, transverse mixing and desired spray cone angle), are energy consuming as well or restricts the choice to a less efficient atomizer designs. Breakup mechanism and spray development in the effervescent atomization have been intensively studied in past two decades however deeper insight into the atomization process and its energy transfer is important for continuing advancement of the atomization performance.

Effectiveness of conversion of input energy into the increased surface energy of the atomized liquid can be quantified with atomization efficiency, η_a. Knowledge of the atomization efficiency is useful for comparison of different types of atomizers and it also enables optimizing atomizer operation conditions for desired spray quality. Basic information on atomization efficiency of different atomizers can be found in the book of Bayvel and Orzechowski [11]. The efficiency of atomization for all traditionally used atomizers is very small, namely $\eta_a < 0.1\%$. Spray quality improvement requires disproportionally more energy due to a drop in the atomization efficiency. Pressure atomizers work with $\eta_a = 0.05 - 0.07\%$ generating droplets with a diameter of 100 μm and several thousandths of a per cent for 50 μm droplets. The efficiency of atomization process of pressure atomizers is commonly higher than that of the pneumatic atomizers [11]. Pneumatic (alias twin-fluid) atomizers use gas to support the atomization process and different forms of these atomizers utilize the gas energy in different ways [12, 13]. Effervescent atomizers, as a subclass of the internally mixed twin-fluid atomizers, are generally supposed to work with the atomization efficiency superior to their fellows, however the statement that atomization efficiency of effervescent atomizers is substantially higher than the efficiencies of pressure, rotary, and most types of twin-fluid atomizers [14] seems to be too optimistic and it is in contrast with [11].

Low energy consumption of effervescent atomizers was recognised already by Chawla [5] in slurry spraying. Several other papers [1, 5, 12, 15, 16] deal with energy considerations of the effervescent atomization but no systematic study dedicated to a detailed description of energy conversion process in effervescent atomization and direct comparison of atomization efficiency of different atomizer types was found. In this paper, we address the issue of energy transfer processes during internal flow, discharge and formation of an effervescent spray. Quali-

* Corresponding author: jedelsky@fme.vutbr.cz

tative explanation of mechanisms involved in the atomization is supported with simple physical equations that describe the energy balance. Data acquired during our earlier investigations of a single-hole effervescent atomizer using Phase Doppler Anemometry (PDA) [1] are used to give numerical results.

General Energy Considerations and Energy Ratios in Effervescent Atomization

Atomization of liquids is a complex energy conversion process accompanied with transformation amongst several energy types. General energy equation for steady one-dimensional homogeneous equilibrium flow without mass and energy conservation in some point of an atomizer can be written as:

$$dq + de + di + \frac{dw^2}{2} + gdz - vdp + \sigma da = 0 \tag{1}$$

where q is heat transfer (e.g. heat energy input to preheat high-viscosity liquids [4] or to preheat liquids for supercritical or flash-boiling atomization, etc.), e is a general symbol for any other input energy source required for given atomization device (e.g. electric energy for ultrasonic and electrostatic atomizers, mechanical power for rotary atomizers), i is the mixture enthalpy, g is gravitational acceleration and the term $-v.dp$ is related to the input pressure energy and it also represents an expansion work) and the last term characterises a change in the surface area of liquid. These energies are related to unit mass of the fluid (liquid or gas-liquid mixture).

Eq. (1) is general and applicable for most of the atomizer types. The potential energy term ($g.dz$) may be neglected in majority of the atomization techniques and also the terms dq and de are not important for our particular case of twin-fluid atomization of light heating oil (LHO) using air in cold (non-reacting) spray considering adiabatic flow conditions. LHO is non-evaporating/non-condensing and original surface energy of bulk liquid is also negligible. Input energy in pneumatic atomization (airblast, effervescent, Y-jet and others) covers the pressure energy of pumped liquid and pressurised atomizing gas.

Energy ratios in effervescent atomization are documented in Table 1 for several sets of input parameters. The energy terms are related to the total input energy. A share of input energy of compressed gas on the total input energy, e_{pg1}, increases with GLR from 88 % at GLR = 0.01 to 99 % at GLR = 0.1. The input energy is partially transformed into kinetic energy and into surface energy of the internal two-phase flow. Relative kinetic energy of the mixture inside mixing chamber (e_{k1}), with maximum about 0.03 % for inlet gauge pressure p_1 = 0.1 MPa and GLR = 0.01, is negligible. Relative surface energy of bubbles/foam inside the mixing chamber, e_{a1}, is in fraction of per cent and decreases with pressure. Fundamental part of the input pressure energy is converted into kinetic energy of discharged two-phase mixture. It is then partially transferred to the momentum of surrounding gas [17], into expansion work when the gas expands out of the atomizer, and some part also remains with the moving dispersed gas-droplet flow. Kinetic energy of the spray is calculated according Eqs. (2) and (3) for data from atomizer E34 [1] measured using PDA in axial distance of 100 mm from the exit orifice. Remaining kinetic energy in this distance is already very low. Relative energy of flowing gas is only 0.05 % of the total input energy at p_1 = 0.5 MPa and GLR = 10 %. It increases with GLR and with input pressure. Relative energy of moving droplets shows an opposite tendency with maximum values in units of per cents at low pressures and low GLRs. Small fraction of input energy is transferred to the increase of droplet surface. Relative surface energy of droplets ($e_{a3} = \eta_a$ = atomization efficiency, addressed in the last section) depends on pressure and GLR with maximum 0.14 % for p_1 = 0.1 MPa and GLR = 1 %. Relative expansion work of the gas, a_3, is about 20 – 30 % depending on the input pressure. Most of the input energy ends converted to turbulent internal/external flow and mixing of the viscous two-phase fluid, shear and frictional losses on passage walls, losses during choked discharge and transferred momentum to the surrounding atmosphere.

Kinetic energy of the discharged mixture can be estimated separately for the gas and liquid phase using PDA data. Gas kinetic energy per mass unit is:

$$e_{kg3} = \frac{E_{kg3}}{m} = \frac{0.5}{1+1/GLR} \sum_{j=1}^{m} r_j w_{gj}^3 \Bigg/ \sum_{j=1}^{m} r_j w_{zgj} \tag{2}$$

where r_j is radial distance from atomizer axis and w_{gj} is mean gas velocity in the position j. Constant gas density, axially symmetrical spray and equidistant sampling distance $\Delta r_j = r_j - r_{j-1}$ are supposed. The gas velocity is calculated as $w_{gj} = \frac{1}{n}\sum_{i=1}^{n_j} w_{dij}$, using values of individual droplet velocity w_{di} as estimate of the gas velocity; only droplets with Stokes number Stk << 1 are included. Kinetic energy of liquid related to the unit mass is:

$$e_{kl3} = \frac{E_{kl3}}{m} = \frac{0.5}{1+GLR} \sum_{j=1}^{m} r_j \sum_{i=1}^{n_j} D_{ij}^3 w_{dij}^2 \Bigg/ \sum_{j=1}^{m} r_j \sum_{i=1}^{n_j} D_{ij}^3 \tag{3}$$

where D_{ij} is diameter of individual droplet i in position j and w_{dij} is its velocity.

Table 1 Energy balance in effervescent atomization, atomizer E34 [1] operated with LHO[f] and air.

p_1 MPa	GLR -	e_{pg1} [a] %	e_{pl1} [a] %	e_{k1} [b] %	e_{a1} [c] %	e_{kg3} [d] %	e_{kl3} [d] %	e_{a3} [d] %	a_3 [e] %
0.1	0.01	88.4	11.6	0.030	0.0111	-	-	0.137	30.5
0.1	0.02	93.9	6.1	0.031	0,0117	0.012	1.229	0.078	32.0
0.1	0.05	97.4	2.6	0.027	-	0.026	0.509	0.035	32.3
0.1	0.1	98.7	1.3	0.021	-	0.033	0.222	0.019	31.2
0.3	0.01	88.4	11.6	0.015	0.0028		-	0.074	30.2
0.3	0.02	93.9	6.1	0.012	0.0029	0.035	1.025	0.042	31.8
0.3	0.05	97.4	2.6	0.009	-	0.040	0.381	0.019	32.0
0.3	0.1	98.7	1.3	0.006	-	0.035	0.185	0.010	31.0
0.5	0.01	88.4	11.6	0.009	0.0012	-	-	0.052	25.9
0.5	0.02	93.9	6.1	0.007	0.0013	0.041	0.854	0.029	27.3
0.5	0.05	97.4	2.6	0.004	0,0013	0.048	0.374	0.013	27.5
0.5	0.1	98.7	1.3	0.003	-	0.052	0.194	0.007	26.6

a based on measured data, calculated according Eqs. (7-10)
b calculated using a discharge model proposed in [1]
c calculated for bubbly flow using Eq. (5), bubble diameter D_b = 3.5 mm (average value from [18-20])
d based on PDA results in spray, calculated according Eq. (2-3)
e calculated for isothermal expansion, energy transfer to the liquid and surrounded air is not taken into account
f physical properties of LHO: density ρ_l = 874 kg/m^3, liquid/gas surface tension σ = 0.0297 kg/s^2

Fluid Mixing and Internal Two-Phase Transport

The atomization process actually starts with the introduction of gas into the liquid inside the mixing chamber. Interaction between gas and liquid differs depending on GLR and moderately also on the input pressure as seen in the Baker's map for the vertical flow [21] (Fig. 1). The mixing chamber is not long enough to allow the flow to fully develop, however the map can give the first idea about the flow character. Qualitatively different mixture forms at low GLR and at high GLR [22]. Bubbly flow, present at low GLR, changes to slug, churn, annular and finally to dispersed flow with GLR increase. Flow regime significantly influences the breakup process and resulting spray.

At low GLR the gas enters the liquid with low velocity. Slowly flowing liquid acts on the penetrating gas calotte and when drag force overcomes the surface tension, σ, the calotte is tiered off forming a bubble. Bubble size depends on surface tension, fluid densities and their velocities [22, 23]. Entry gas velocity is governed by the size of the aeration holes and operation conditions. Velocity of liquid prior to mixing depends on the ratio of cross-sections of the mixing channel and exit orifice and the operation conditions. Also geometric arrangement of the aerator influences the two-phase formation. The bubbles can agglomerate or breakup during the flow [22], though Huang *et al.* [24] observed relatively steady bubbly flow with only few bubbles coalescing. Their chaotic - turbulent motion towards the exit orifice promotes mixture homogeneity, however gas-liquid separation can appear for horizontal flows [25]. Bubble shape depends on its size. Small bubbles tend to reach spherical shape while larger bubbles elongate and warp due to pressure fluctuations in turbulent flow. The bubbly flow can develop only if:

$$GLR \le c\frac{\rho_{g1}}{\rho_l} = c\frac{p_{g1} + p_b}{\rho_l RT} \tag{4}$$

where ρ_{g1} and ρ_l are gas and liquid densities, p_{g1} is gas gauge pressure upstream the exit orifice, R is specific gas constants and T is temperature of the mixture. The constant c depends on structure of the bubbly flow. A mixture containing spherical monodisperse bubbles uniformly arranged in simple cubic pattern gives $c = \pi/(6-\pi)$. Bubbly flow regime for the most effective geometrical configuration of monodisperse bubbles is given by $c = 2.85$ or for polydisperse bubbles by $c = 4.6$ according Lefebvre [12]. Bubbly flow limits calculated for the last c value fit the best with experimental results of Huang *et al.* [24]. Using LHO physical properties (from Table 1) and air at room temperature in Eq. (4) leads to GLR ≤ 6.2 p [%, MPa]. Note that for fully developed flow of pure liquids the bubbly flow conditions are fulfilled if the void fraction is lower than about 10 % [26]; void fraction for real bubbly flow observed in [24] and predicted by Eq. (4) for $c = 4.6$ is much higher than 10 % which suggests the flow cannot fully develop. Larger and more numerous bubbles form with increase in the gas

amount. The bubbles can eventually reach the size of the channel diameter. Such slug flow, characterised with intermittent discharge of dominant fraction of one phase, causes an undesired fluctuating spray [25]. Further gas increase leads to increase in the flow velocity; the mixture is frothy or churn and it is more homogeneous than in the previous case. Continuing increase in gas fraction changes the flow to annular, all liquid flows on the channel wall while gas occupies central part of the channel. The fast flowing gas pulls down the slowly flowing liquid, waving its surface and eventually also forming droplets. The interfacial area A_b increases with GLR for bubbly flow, with the bubble surface energy per unit mass of the mixture, m:

$$e_{ab} = \frac{E_{ab}}{m}\frac{\sigma A_b}{m} = \frac{6\sigma}{\rho_{g1}\overline{D_b}}\frac{GLR}{(GLR+1)} \tag{5}$$

where the average bubble size $\overline{D_b} = D_{b20}$. Situation is more complicated for slug and churn flow and for annular flow this area reduces with GLR because of a simple cylindrical interface between gas and liquid.

The mixing process is, in the simplest case of equal input temperature of gas and liquid, practically isothermal. Input gas pressure, p_{g1}, differs from the liquid pressure, p_{l1}, only to allow gas to flow through aeration holes; $\Delta p_1 = p_{g1} - p_{l1}$ is typically in kPa rate [25]. Energy related to the pressure difference transforms into heat due to friction losses and into surface energy of the mixture. Small pressure difference along the mixing channel is needed to overcome wall friction and resistance of the turbulent motion of the two-phase mixture. These effects spend only small fraction of the input energy, However the mixture formation is very important for the resulting spray; size of produced droplets is proportional to the square root of the initial thickness or diameter of the ligaments from which they were formed [27].

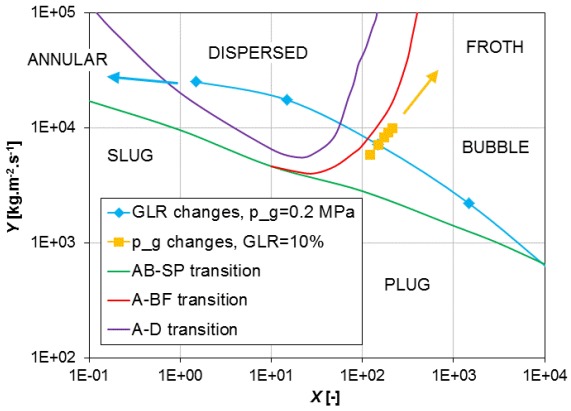

Figure 1 Modified Baker's map for vertical downward two-phase flow with transformed coordinates according to [21] with marked influence of operational conditions on the two-phase flow regime. Arrows show direction of regime change while the appropriate values increase. AB-SP: line defining transition between bubble and plug or annular and slug pattern, A-BF: annular/bubble-froth pattern transition, A-D: annular/dispersed pattern transition. The atomizer is operating with air and LHO, d_c = 8 mm, d_o = 2.5 mm.

Two-Phase Discharge and Liquid Breakup

The mixture accelerates due to cross section reduction (Bernoulli principle) which leads to bubble elongation [15, 28] and expansion controlled by the pressure drop. It causes further increase in interfacial surface. Liquid membranes, filaments and ligaments are formed [29]. This phase corresponds well to the film formation in the case of prefilming atomizers or pressure-swirl atomizers although it is managed different ways. Gas bubbles expand and finally explode [18, 30] causing ligament thinning and disruption. The gas flows with higher velocity (choked flow if critical pressure ratio achieved [1] and it acts on the liquid ligaments similar way as in the case of airblast prefilming atomization. This velocity slip results in acceleration of the liquid mass followed with continuing transformation of the bulk liquid into shreds and ligaments and with a surface wave formation which enhances the atomization process. The gas-liquid interaction influences the liquid instability in the near-nozzle region. The drag between the gas and liquid causes a small decrease in the air velocity [31].

At very low GLR, about 0.1 %, and low pressure 0.01 MPa the liquid forms a continual film and ligaments at the nozzle exit (Fig. 2). The thin ligaments disintegrate due to surface tension and wrap into droplets. Primary breakup proceeds through a distance of several nozzle diameters. Increase of GLR promotes disintegration of the liquid volumes and shortens the breakup distance. At GLR > 2 % no compact liquid volume is observed; the two-phase mass already in vicinity of the exit orifice contains a cloud of small particles too optically dense to look through, however we assume that also at higher GLR a liquid core exists at the nozzle exit as documented by ballistic imaging [30]. The atomization process, in the case of annular or dispersed internal two-phase flow, relies on the aerodynamic shear force.

The gas-liquid mixture is spatially homogeneous only in the case of low GLR, where bubbly flow appears. Relatively uniform droplet size in radial profile is generated in this case as seen in [32] and [33]. Mixture in slug or annular flow regime is more heterogeneous [34]. The gas occupies mainly inner part of the flow channel and liquid is attached to the channel walls due to adhesive forces. This uneven gas distribution means that the gas pressure energy is concentrated near the exit orifice centreline where it enhances the breakup while atomization

out of the centreline suffers from lack of the gas leading to larger droplets [28]. Radial size profile with distinct minimum near the spray centreline and maximum at the spray borders as observed in [1, 35] results from this phenomena.

Intensity in the momentum transfer between the gas and liquid inside the exit hole can be estimated by comparing real discharge characteristics with predictions by analytical models of two-phase discharge. We have done this comparison for a set of 26 single-hole effervescent atomizers with outside-in gas injection operating with LHO in range of pressures 0.1 - 1 MPa and GLR = 0.01 – 1 [1] and have found real discharge coefficient just in the middle of the two extreme cases of gas-liquid discharge: (1) without slip between the gas and liquid phases (Homogeneous Flow Model = HFM) and (2) discharge with maximum slip between the phases respectively (Separated Flow Model = SFM) irrespective of the pressure and GLR.

The velocity slip between gas and liquid phase, which is very small for bubbly flow and large for annular flow inside the mixing chamber, increases in the constricted exit orifice. Gas accelerates and reaches the highest velocity in the smallest cross section for non-choked conditions or near behind it for choked conditions. Momentum transfer between gas and liquid accelerates the liquid; small liquid fragments reach higher velocity than large filaments oriented mostly parallel to the flow. Expanding gas decelerates with distance from exit orifice. Formed droplets keep momentum of the parent liquid fragments so in large distances from the orifice large droplets are faster than surrounding air while velocity of small droplets corresponds to the air velocity. Mixing with surrounding air also decelerates the spray. The discharge process thus leads to interesting spatially variable velocity distribution of the gas and liquid, where certain positive or negative correlation between the velocity and liquid phase size appears depending on radial and axial distance from the nozzle exit (Fig. 3 right). Trajectory of large particles follows well the direction given during discharge. Motion of small particles is dictated by the gas turbulent flow which leads to their dispersion and enhances transversal mixing [36]. It results in twin-peak size distribution in large radial distances, as seen in [37], and also contributes to droplet collisions and coalescence.

0.01 MPa, 0.1 % 0.02 MPa, 0.3 % 0.05 MPa, 1 % 0.1 MPa, 5 % 0.2 MPa, 10 %

Figure 2 Spray structure of effervescent atomizer at varying air gauge pressure and GLR.

The interfacial area A_b increases with GLR for bubbly flow, with the bubble surface energy per unit mass of the mixture, m:

$$e_{ad} = \frac{E_{ad}}{m} = \frac{\sigma A_d}{m} = \frac{6\sigma}{\rho_l \overline{D_d}} \frac{1}{(GLR+1)} \tag{6}$$

where the average droplet size $\overline{D_d} = D_{d20}$. For a ratio between surface energy of final droplets and surface energy of the bubbles in the internal flow using Eq. (5) and Eq. (6) we obtain: $\frac{e_{ad}}{e_{ab}} = \frac{\rho_{g1}}{\rho_l} \frac{D_{b20}}{D_{d20}} \frac{1}{GLR} \approx \frac{p_{g1} + p_b}{GLR}$. This ratio is in order of 10 for GLR = 0.01 (see Table 1).

Expansion cooling during discharge causes temperature of the liquid drops down; but several °C only (Fig. 3 left). It is due to high liquid specific heat capacity compared to the gas specific heat capacity. Very fast discharge moreover does not allow for intense heat transfer and cooling of the liquid by expanding gas. Note that the IR camera performs a "temperature averaging" over the spray thickness so it gives an approximate image of the temperature distribution. The lowest temperature is achieved near the nozzle exit with consequent temperature relaxation as the surface temperature equalises through the droplet volume.

Atomization Efficiency

Atomization efficiency is given by a ratio of the surface energy of droplets in the spray, E_a, and the total energy E_i required to produce the spray. The term E_i in twin-fluid atomization consists of energy introduced by the

pressurized gas, E_g, and energy of the supplied liquid, E_l [5, 15]. Isothermal compression energy needed to pressurize the gas mass M_g from atmospheric pressure p_b to the pressure $p = p_g + p_b$ in front of the nozzle reads:

$$E_g = \frac{m_g}{\rho_{gb}} \cdot p_b \cdot \ln\left(\frac{p_{g1}+p_b}{p_b}\right) = V_{gb} \cdot p_b \cdot \ln\left(\frac{p_{g1}+p_b}{p_b}\right) = V_{g1} \cdot \left(p_{g1}+p_b\right) \cdot \ln\left(\frac{p_{g1}+p_b}{p_b}\right) \tag{7}$$

where ρ_{gb} is gas density at atmospheric pressure, V_{gb} is gas volume at atmospheric pressure and V_{g1} is volume of the pressurized gas. The potential energy of the supplied liquid, in accordance with [15], reads:

$$E_l = m_l \cdot \frac{p_{l1}}{\rho_l} = V_l \cdot p_{l1}. \tag{8}$$

Using Eqs. (7) and (8) and definition equation for gas-to-liquid-ratio:

$$GLR = m_g / m_l = \left(V_{g1} \cdot \rho_{g1}\right) / \left(V_l \cdot \rho_l\right) \tag{9}$$

we can write:

$$E_i = E_g + E_l = V_l \cdot \left[p_{l1} + GLR \cdot \frac{\rho_l}{\rho_{g1}} \cdot \left(p_{g1}+p_b\right) \cdot \ln\left(\frac{p_{g1}+p_b}{p_b}\right)\right]. \tag{10}$$

Transformation of bulk liquid into fine droplets is associated with enormous increase of surface. After fragmentation of bulk liquid with volume V_l into droplets having all the same diameter ID_{20} (so called Integral surface diameter) the area of the droplet system will be $A_d = 6 \cdot V_l / ID_{20}$. The diameter ID_{20} can be estimated using PDA data as $ID_{20} = \sum_{j=1}^{m} r_j \sum_{i=1}^{n_j} D_{ij}^2 \Big/ \sum_{j=1}^{m} r_j n_j$. The corresponding surface energy increase (neglecting original surface energy of bulk liquid) reads $E_{ad} = A_d \cdot \sigma$ [38]. The atomization efficiency is thus:

$$\eta_a = \frac{E_a}{E_i} = \frac{6 \cdot V_l \cdot \sigma / ID_{20}}{E_i} = \frac{6 \cdot \sigma / ID_{20}}{p_{l1} + GLR \cdot \frac{\rho_l}{\rho_{g1}} \cdot \left(p_{g1}+p_b\right) \cdot \ln\left(\frac{p_{g1}+p_b}{p_b}\right)}. \tag{11}$$

Efficiency of effervescent atomization, shown in Fig. 4 left for varying inlet pressure and GLR, is less than 0.1 % for common operation conditions of the atomizer. As suggested by the log-log scale of the plot, there is approximately inverse logarithmic tendency of the η_a with GLR and similar trend was found also for pressure. Increase in the pressure and GLR promotes atomization reducing Sauter mean diameter, D_{32}, as well as D_{20}. However atomization efficiency drops down and it means that the input gas and liquid energy is utilized less effectively. Note that similar behaviour was found for airblast atomizers [16] and explained by increased gas/liquid separation which reduces the fraction of gas that participates on the breakup process. Our findings justify the Lefebvre's suggestions to operate effervescent atomizers at bubbly flow regime requiring low gas consumption. Fig. 4 right shows that η_a for effervescent atomizers is lower than η_a for pressure atomizers which is in accordance with [11]. It also follows from Fig. 4 left considering GLR = 0 for pressure atomizers. It disproves the statement about superior η_a of effervescent atomizers compared to pressure atomizers in [14]. Atomization efficiency of effervescent atomizers generally decreases with a requirement of smaller droplets; atomization at high pressures produces spray of the same quality more effectively. Regardless worse η_a of effervescent compared to pressure atomization, its main advantage can be seen in possibility to acquire the spray of the same quality at much lower pressure. Larger clear area of exit orifice of the effervescent atomizers protects them from clogging and

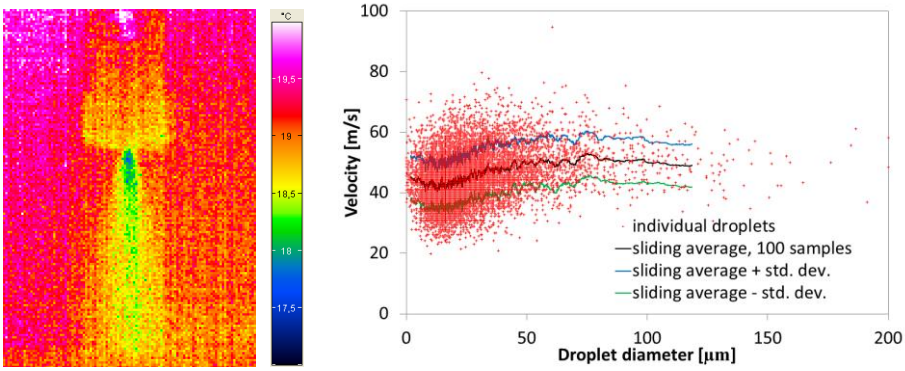

Figure 3 (left) Thermovision snapshot of the effervescent spray. **(right)** Size – velocity correlation, p = 0.3 MPa, GLR = 2 %, r = 0 mm, z = 100 mm.

makes them useful for waste liquids. They generate droplets of given size with higher efficiency then other types of twin-fluid and especially of the airblast atomizers [39].

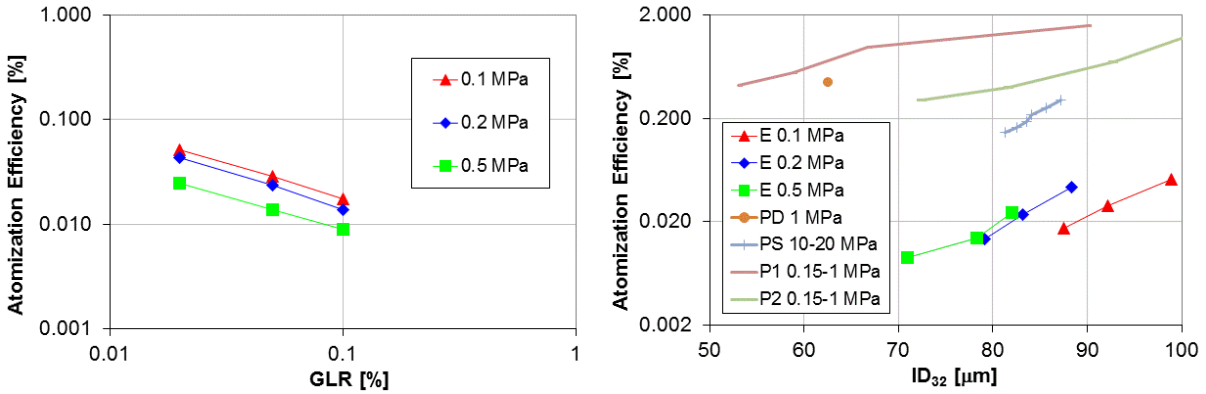

Figure 4 (left) Atomization efficiency of effervescent atomizer at varied operation pressure and GLR. **(right)** Atomization efficiency of different atomizer types with regard to produced ID_{32}: e - effervescent atomizer with orifice diameter D_o=2.5 mm, operated with LHO/air; PS – pressure-swirl atomizer with D_o=2.8 mm, LHO; PD – simplex atomizer with D_o=0.4 mm, LHO; P1 – new design of pressure-swirl atomizer with D_o=0.36 mm, Kerosene; P2 – old design of pressure-swirl atomizer with D_o=0.36 mm, Kerosene.

Summary and Conclusions

The paper considers the effervescent atomization as an energy conversion process which starts with the gas injection into the liquid and results in far-nozzle motion of droplets. Mechanisms involved in the two-phase mixture formation during internal flow, discharge and spray formation were qualitatively described based on own experimental results and available literature data.

Our estimation of the energy balance in effervescent atomization shows that the gas/liquid surface formation process during internal mixing as well as during the discharge consumes minor part of the input energy. Most of the input energy is spent to expansion work of the discharged gas, air entrainment process and losses related to the two-phase flow and discharge. Atomization efficiency depends on operation conditions of the atomizer and declines with an increase in GLR and with increase in input pressure. It is always lower than efficiency of pressure atomizers for comparable conditions.

Acknowledgements

Authors greatly acknowledge financial support from project No. 101/11/1264 funded by the Czech Science Foundation and from „NETME centre - New Technologies for Mechanical Engineering" Reg. No. CZ.1.05/2.1.00/01.0002.

References

[1] Jedelsky J, Jicha M, Slama J, Otahal J. Development of an Effervescent Atomizer for Industrial Burners. Energy & Fuels 2009;23:6121-30.

[2] Buckner HN, Sojka PE, Lefebvre AH. Effervescent atomization of coal-water slurries. ASME Publ., 1990; pp. 105–8.

[3] Loebker D, Empie HJ, Tappi. Effervescent spraying: A new approach to spraying high solids black liquor. TAPPI International Engineering Conference. Miami, Fl, 1998; pp. 157-67.

[4] Kermes V, Belohradsky P. Experimental study on combustion of liquid renewable fuels. Pres 2010: 13th International Conference on Process Integration, Modelling and Optimisation for Energy Saving and Pollution Reduction 2010;21:457-62.

[5] Chawla JM. Atomization of Liquids Employing the Low Sonic Velocity in Liquid/Gas Mixtures. Proceedings of the Third ICLASS-85, 1985; pp. LP/1A/5/1-LP/A/5/7.

[6] Lefebvre AH, Wang XF, Martin CA. SPRAY CHARACTERISTICS OF AERATED-LIQUID PRESSURE ATOMIZERS. Journal of Propulsion and Power 1988;4:293-8.

[7] Wade RA, Weerts JM, Sojka PE, Gore JP, Eckerle WA. Effervescent atomization at injection pressures in the MPa range. Atomization and Sprays 1999;9:651-67.

[8] Mujumdar AS, Huang LX, Chen XD. An overview of the recent advances in spray-drying. Dairy Science & Technology 2010;90:211-24.

[9] Esfarjani SA, Dolatabadi A. A 3D simulation of two-phase flow in an effervescent atomizer for suspension plasma spray. Surface & Coatings Technology 2009;203:2074-80.

[10] Loebker D, Empie HJ. High mass flow-rate effervescent spraying of high viscosity Newtonian liquid. the 10th Annual Conference on Liquid Atomization and Spray Systems. Ottawa, ON, 1997; pp. 253-7.
[11] Bayvel L, Orzechowski Z. Liquid Atomization: Taylor & Francis Inc., 1993.
[12] Lefebvre AH. TWIN-FLUID ATOMIZATION: FACTORS INFLUENCING MEAN DROP SIZE. Atomization and Sprays 1992:101-19.
[13] Chin JS. EFFERVESCENT ATOMIZATION AND INTERNAL MIXING AIR ASSIST ATOMIZATION. International Journal of Turbo & Jet-Engines 1995;12:119-27.
[14] Sovani SD, Sojka PE, Lefebvre AH. Effervescent atomization. Progress in Energy and Combustion Science 2001;27:483-521.
[15] Lörcher M, Schmidt F, Mewes D. Flow Field and Phase Distribution Inside Effervescent Atomizers. 9th ICLASS 2003, 2003; pp. 12-9.
[16] Lefebvre AH. ENERGY CONSIDERATIONS IN TWIN-FLUID ATOMIZATION. Journal of Engineering for Gas Turbines and Power-Transactions of the Asme 1992;114:89-96.
[17] Bush SG, P. E. Sojka. Entrainment by Effervescent Sprays at Low Mass Flowrates. *Proc of the 6th ICLASS*, 1994; pp. 609-15.
[18] Gadgil HP, Raghunandan BN. Some features of spray breakup in effervescent atomizers. Experiments in Fluids 2011;50:329-38.
[19] Jedelsky J, Jicha M. Unsteadiness in effervescent sprays: A new evaluation method and the influence of operational conditions. Atomization and Sprays 2008;18:49-83.
[20] Jagannathan TK, Nagarajan R, Ramamurthi K. Effect of ultrasound on bubble breakup within the mixing chamber of an effervescent atomizer. Chemical Engineering and Processing 2011;50:305-15.
[21] Process Associates of America. Modified Baker's map for horizontal two-phase flow with transformed coordinates. Available at: http://www.processassociates.com/process/fluid/2faz_xy.htm Acessed March 2003.
[22] Shepard TG. Bubble Size Effect on Effervescent Atomization. THE FACULTY OF THE GRADUATE SCHOOL OF THE UNIVERSITY OF MINNESOTA. MINNESOTA: THE UNIVERSITY OF MINNESOTA, 2011; p. 149.
[23] Lefebvre AH. Some recent developments in twin-fluid atomization. Particle & Particle Systems Characterization 1996;13:205-16.
[24] Huang X, Wang X, Liao G. Visualization of two phase flow inside an effervescent atomizer. Journal of Visualization 2008;11:299-308.
[25] Jedelsky J, Jicha M. Characteristics of a Two-Phase Flow Inside the Mixing Chamber of an Effervescent Atomizer. International Symposium on Two-Phase Flow Modelling and Experimentation. Pisa, Italy, 2004.
[26] Wallis G. One Dimensional Two-Phase Flow: Mcgraw-Hill (Tx), August 1969.
[27] Lefebvre AH. *Atomization and Sprays*. Bristol: Tailor & Francis, 1989.
[28] Ramamurthi K, Sarkar UK, Raghunandan BN. Performance characteristics of effervescent atomizer in different flow regimes. Atomization and Sprays 2009;19:41-56.
[29] Santangelo PJ, Sojka PE. A HOLOGRAPHIC INVESTIGATION OF THE NEAR-NOZZLE STRUCTURE OF AN EFFERVESCENT ATOMIZER-PRODUCED SPRAY. Atomization and Sprays 1995;5:137-55.
[30] Linne M, Sedarsky D, Meyer T, Gord J, Carter C. Ballistic imaging in the near-field of an effervescent spray. Experiments in Fluids 2010;49:911-23.
[31] Shavit U. Gas-liquid interaction in the liquid breakup region of twin-fluid atomization. Experiments in Fluids 2001;31:550-7.
[32] Li J, Lefebvre AH, Rollbuhler JR. Effervescent atomizers for small gas turbines. American Society of Mechanical Engineers, 1994; pp. 1–6.
[33] Kufferath A, Wende B, Leuckel W. Influence of liquid flow conditions on spray characteristics of internal-mixing twin-fluid atomizers. International Journal of Heat and Fluid Flow 1999;20:513-9.
[34] Catlin CA, Swithenbank J. Physical processes influencing effervescent atomizer performance in the slug and annular flow regimes. Atomization and Sprays 2001;11:575-95.
[35] Kushari A. Effect of injector geometry on the performance of an internally mixed liquid atomizer. Fuel Processing Technology 2010;91:1650-4.
[36] Luong JTK, Sojka PE. Unsteadiness in effervescent sprays. Atomization and Sprays 1999;9:87-109.
[37] Jedelsky J, Jicha M, Slama J. Characteristics and Behaviour of Multi-Hole Effervescent Atomizers. Proc ILASS-Europe 2004. Nottingham, United Kingdom, 2004; pp. 521–6.
[38] Frohn A, Roth N. Dynamics Of Droplets. Berlin: Springer-Verlag, 2000.
[39] Sher E, Elata C. SPRAY FORMATION FROM PRESSURE CANS BY FLASHING. Industrial & Engineering Chemistry Process Design and Development 1977;16:237-42.